ADVANCED ENERGY MATERIALS

Supporting Information

for *Adv. Energy Mater.,* DOI: 10.1002/aenm.202001440

Lithium Difluorophosphate-Based Dual-Salt Low Concentration Electrolytes for Lithium Metal Batteries

Hao Zheng, Hongfa Xiang, Fuyang Jiang, Yongchao Liu, Yi Sun, Xin Liang, Yuezhan Feng, and Yan Yu**

Supporting Information

Lithium Difluorophosphate-Based Dual-Salt Low Concentration Electrolytes for Lithium Metal Batteries

Hao Zheng, Hongfa Xiang, Fuyang Jiang, Yongchao Liu, Yi Sun, Xin Liang, Yuezhan Feng, and Yan Yu***

H. Zheng, F. Jiang, Y Liu, Dr. Y. Sun, Dr. X. Liang, Prof. H. Xiang
School of Materials Science and Engineering, Engineering Research Center of High Performance Copper Alloy Materials and Processing, Ministry of Education,
Hefei University of Technology
Hefei, Anhui 230009, P.R. China
Email: hfxiang@hfut.edu.cn

Dr. Y. Feng,
Key Laboratory of Materials Processing and Mold (Zhengzhou University),
Ministry of Education, Zhengzhou University
Zhengzhou 450002, P.R. China

Prof. Y. Yu
Hefei National Laboratory for Physical Sciences at the Microscale
Department of Materials Science and Engineering
CAS Key Laboratory of Materials for Energy Conversion
University of Science and Technology of China
Hefei, Anhui 230026, P. R. China
E-mail: yanyumse@ustc.edu.cn

Prof. Y. Yu
Dalian National Laboratory for Clean Energy (DNL)
Chinese Academy of Sciences (CAS)
Dalian 116023, P. R. China

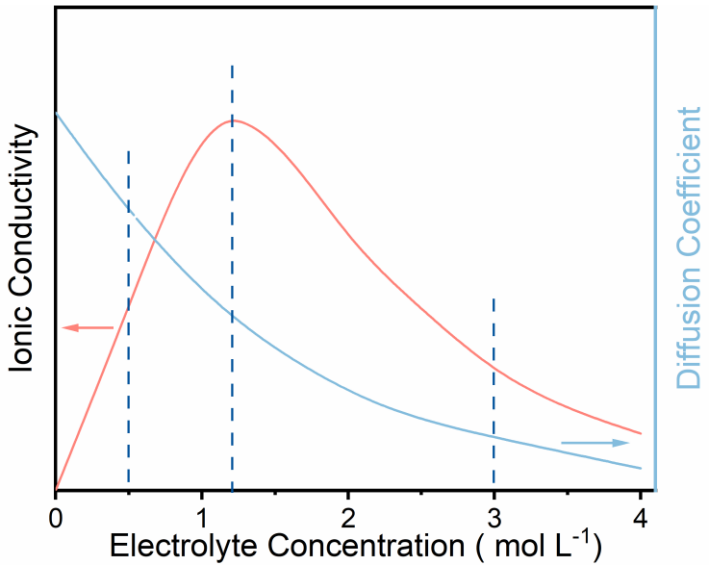

Figure S1. Illustration of influence of salt concentration on ionic conductivity and diffusion coefficient of Li^+.

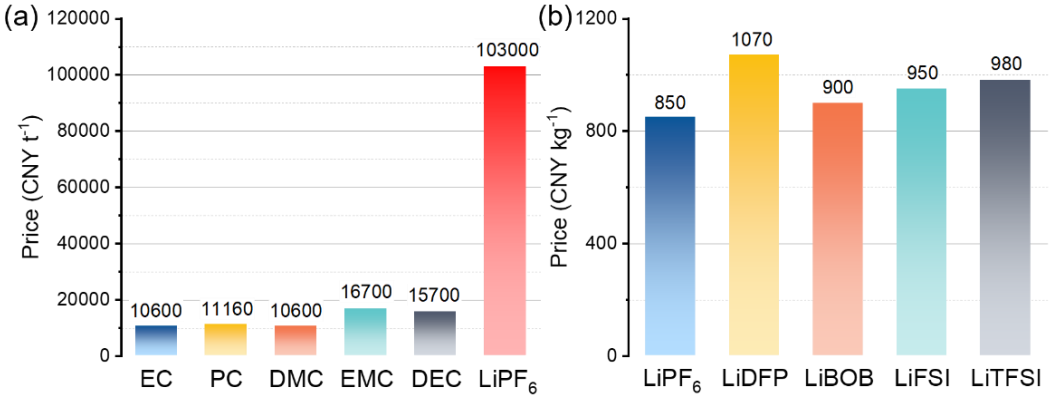

Figure S2. (a) The price of commercial used carbonated solvents and $LiPF_6$ sold in tons and (b) the price of Li salts sold in kilograms.

Table S1. The weight and cost proportion of solvent and salt in 1 dm^{-3} electrolyte.

Component	Weight (g)	Cost (CNY)	Proportion (%)
Solvent	1068.09	13.89	45.9
Salt	151.91	16.39	54.1

Table S2. The salt cost at different concentration in 1 dm^{-3} electrolyte.

Salt	Molecular Weight ($g\ mol^{-1}$)	Concentration ($mol\ dm^{-3}$)	Weight (g)	Unit Price (CNY kg^{-1})	Cost (CNY)
$LiPF_6$	151.91	1	151.91	850	129.1
LiDFP	107.91	0.1	10.79	1070	11.5
LiBOB	193.79	0.4	77.52	900	69.8
LiFSI	187.06	0.4	74.82	950	71.1
LiTFSI	287.09	0.4	114.84	980	112.5

The price of carbonated solvents and $LiPF_6$ sold in tons is shown in Figure S2a. As many salts are not sold in tons due to their lower production capacity and consumption than $LiPF_6$, the price of the salts used in this work is compared in kilograms, which is much expensive than in tons (Figure S2b). Noted that the price is investigated on October 2019 from companies in China and the prices fluctuates over time. The average solvent price of 13000 CHY t^{-1} is used as the unit-price of solvent and the density of the electrolyte is assumed as 1.22 g cm^{-3} (usually the density of the commonly used electrolytes is 1.2~1.3 g cm^{-3}). Due to the high unit-price of Li salt, the cost of $LiPF_6$ accounts for 54.1% of the total cost although the weight ratio of $LiPF_6$ is only 12.5% (Table S1). The total salt cost in 1 dm^{-3} STD, D4B, D4F and D4T electrolyte is 129.1, 81.3, 82.6 and 124.1 CNY (Table S2). Obviously, the salt cost in D4B and D4F electrolyte is much lower than the STD electrolyte. The D4T electrolyte exhibits comparable cost to the STD electrolyte due to the high molecular weight of LiTFSI. Moreover, with the promotion of synthetic technology and extensive applications, the cost of the salts used in LCEs can be further reduced.

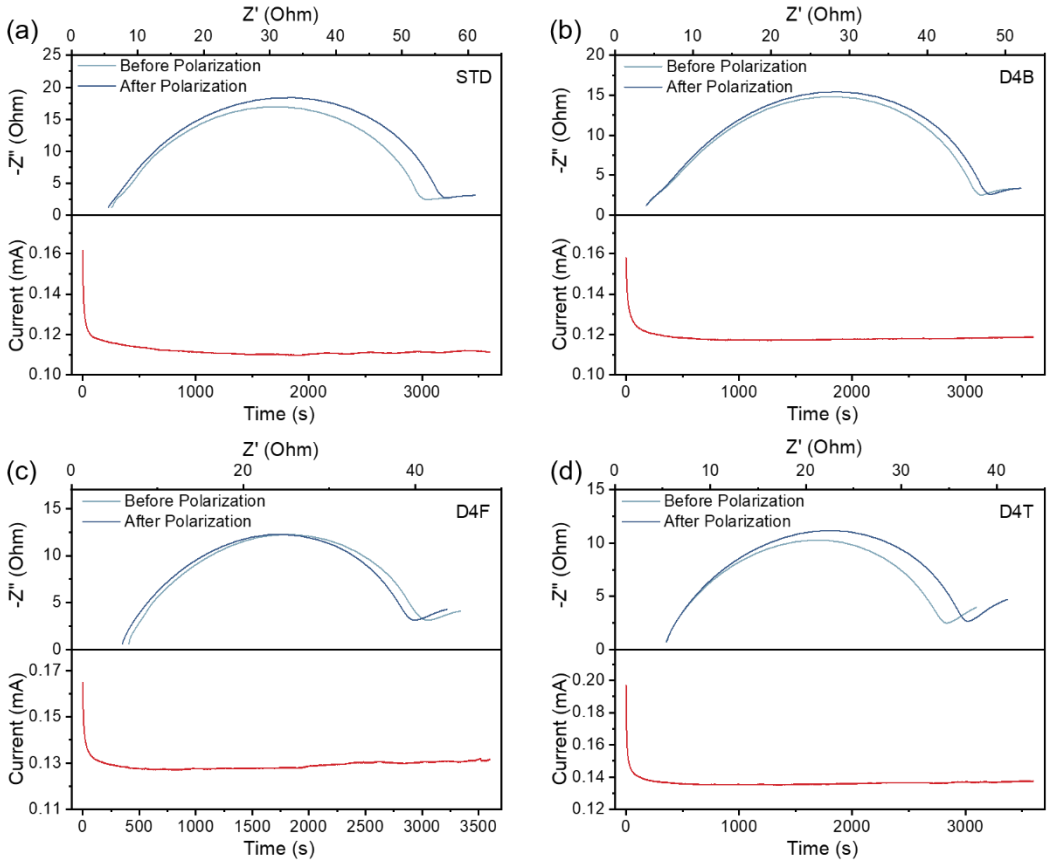

Figure S3. Nyquist and chronoamperometry plots of Li||Li symmetric cells in (a) STD, (b) D4B, (c) D4F and (d) D4T electrolytes.

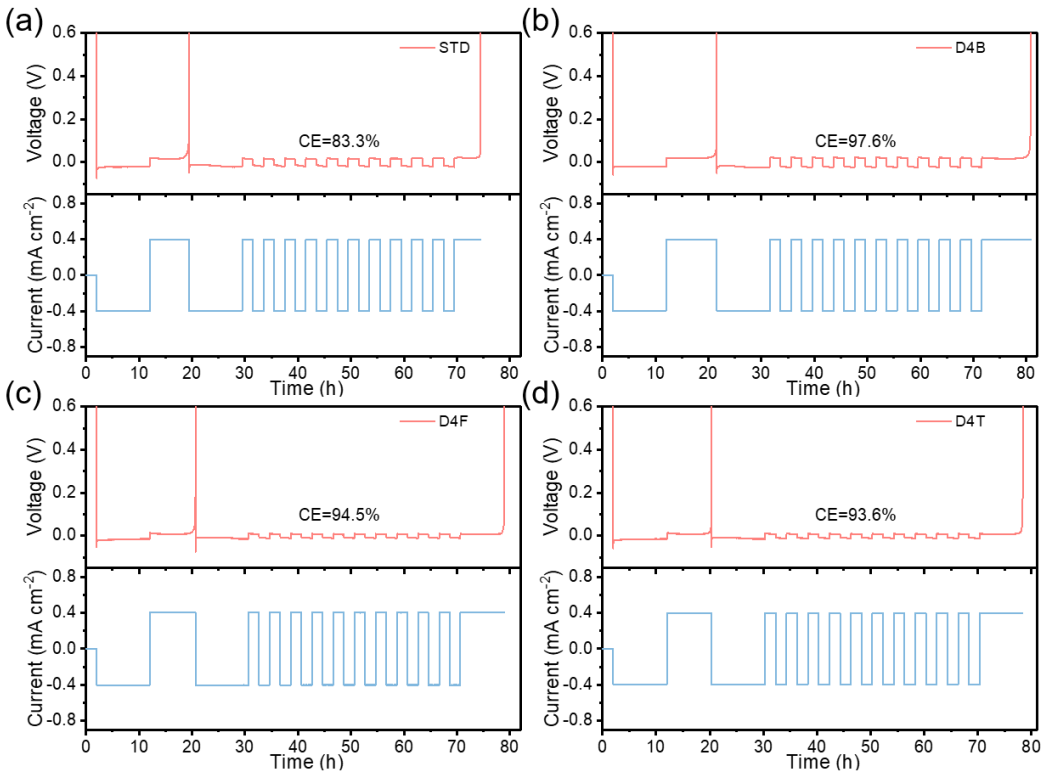

Figure S4. Voltage and current versus time plots of the Li||Cu cells in average CE measurement for (a) STD, (b) D4B, (c) D4F and (d) D4T electrolytes.

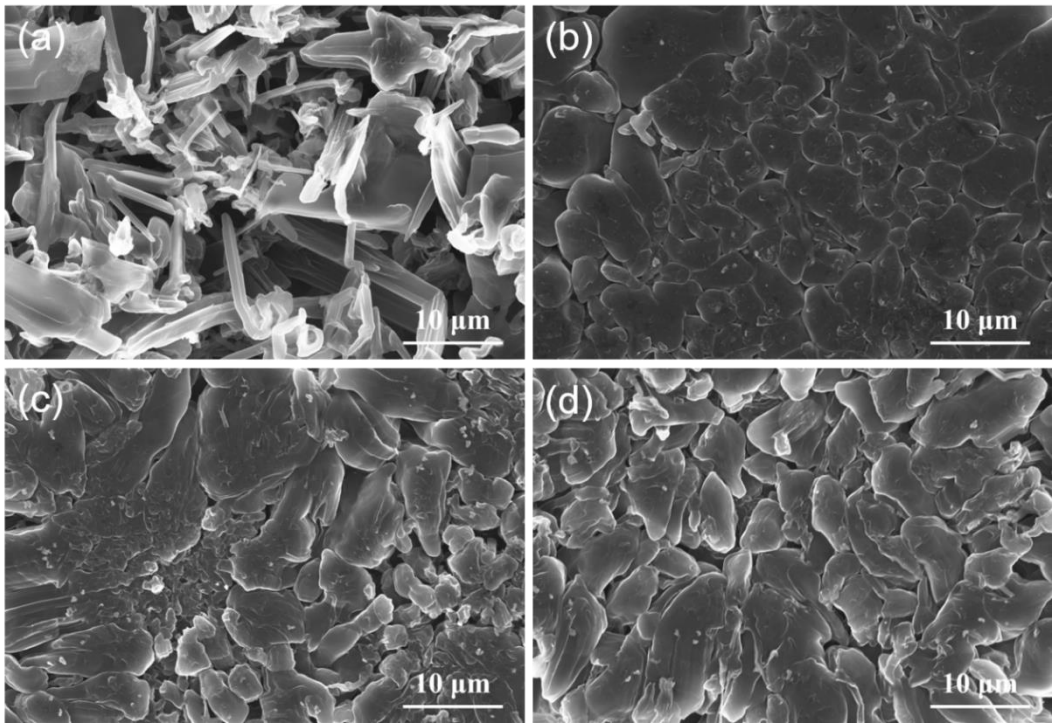

Figure S5. Surface morphologies of the Li deposited on Cu foil with an areal capacity of 1.5 mAh cm^{-2} in (a) STD, (b) D4B, (c) D4F and (d) D4T electrolytes.

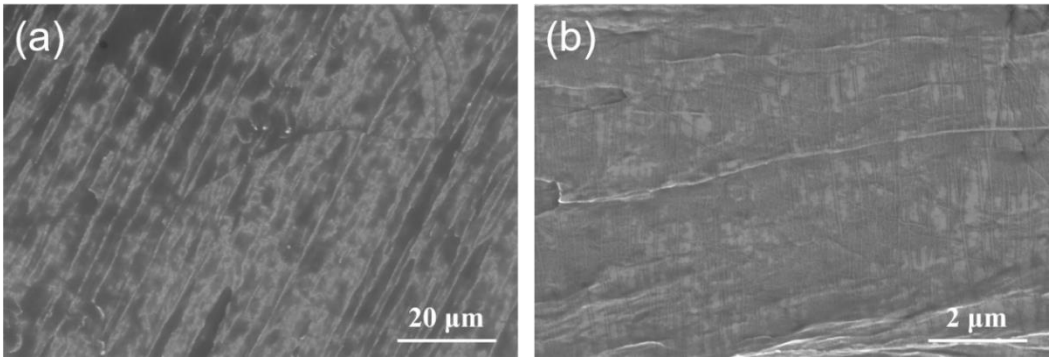

Figure S6. Surface morphologies of pristine Li at different magnifications.

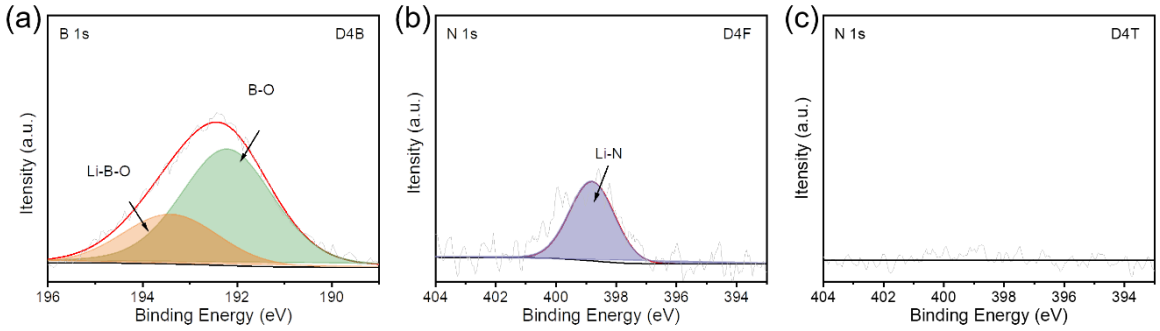

Figure S7. B 1s and N 1s XPS spectra of the Li anode harvested from the Li||Li symmetric cells after cycling in (a) D4B, (b) D4F and (c) D4T electrolytes.

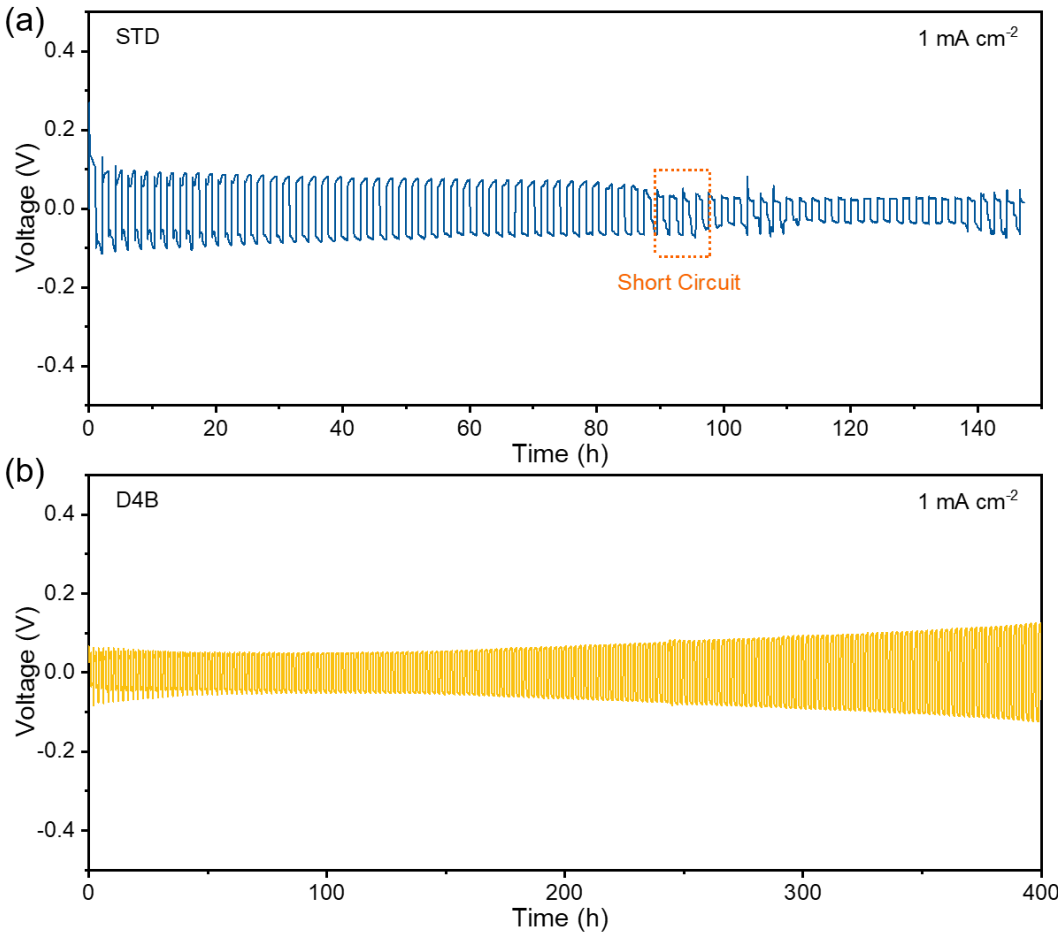

Figure S8. Cycling performance of Li||Li symmetric cells in (a) STD, (b) D4B at 1 mA cm^{-2} and 1 mAh cm^{-2}.

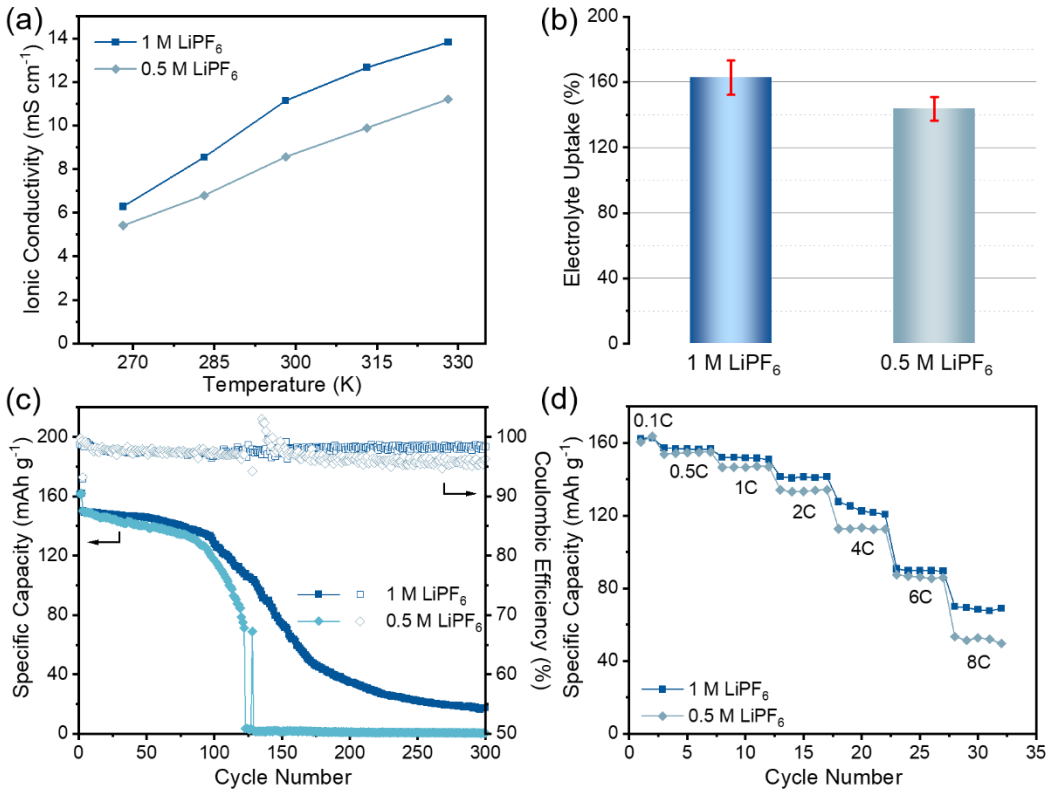

Figure S9. Comparison of the (a) ionic conductivity and (b) electrolyte uptake of 0.5 M and 1 M $LiPF_6$ electrolyte. (c) Cycling and (d) rate performance of the Li||LFP cells in 0.5 M and 1 M $LiPF_6$ electrolyte.

The ionic conductivity, electrolyte uptake, cycling and rate performance of 0.5 M $LiPF_6$ electrolyte are also investigated to illustrate the influence of Li salt concentration on electrolyte characteristics and battery performance more intuitively (Figure S9). The ionic conductivity of 0.5 M $LiPF_6$ electrolyte is lower than 1 M $LiPF_6$ electrolyte, but still higher than LCEs, indicating the good ionic conductivity of $LiPF_6$ electrolyte. With the decrease of salt concentration, the electrolyte uptake decreased a lot, which is lower than all LCEs. Furthermore, the cycling stability and rate performance of the cell using 0.5 M $LiPF_6$ electrolyte are worse compared to STD (1 M $LiPF_6$). This further confirms that it is the SEI layer rather than ionic conductivity that governs the cell performance.

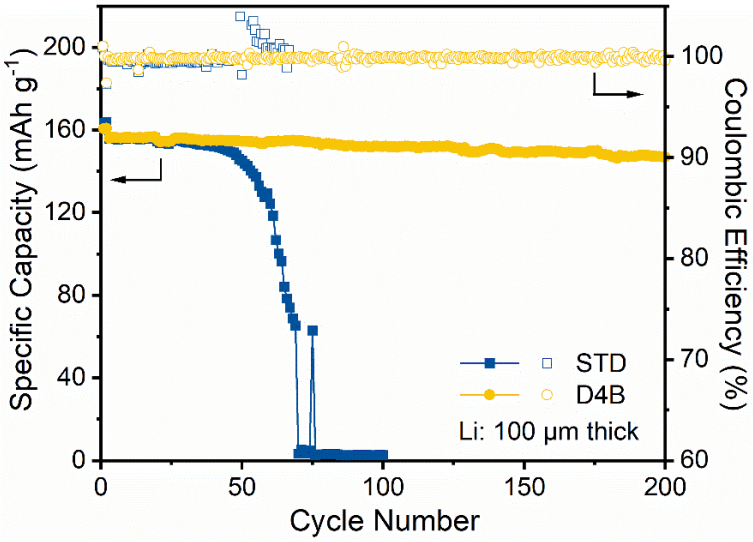

Figure S10. The cycling performance of Li||LFP cells with 100 μm Li foil at 1C.

To further illustrate the practicality of LCE, the performance of STD and D4B electrolyte with a Li foil of 100 μm have been measured (Figure S10). In STD electrolyte, fast capacity degradation is observed after 45 cycles and the cell completely fails only after 70 cycles, which is inferior to the cell using 450 μm Li foil. On the contrary, in D4B electrolyte, the capacity retention reaches 94.2% after 200 cycles with an average CE of 99.8%. Compared with the cells using 450 μm Li, this performance is slightly deteriorated, but it still exhibits significantly enhanced performance in the LCEs.

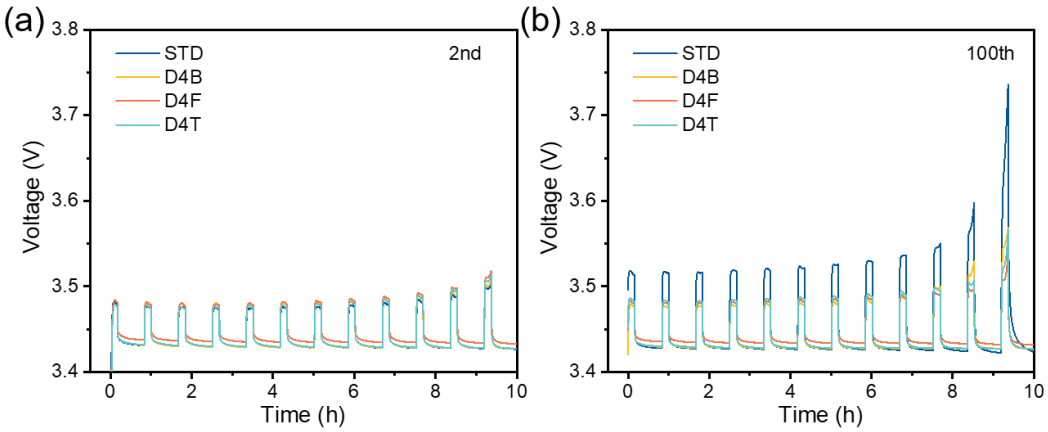

Figure S11. GITT profiles of Li||LFP cells after (a) 2 and (b) 100 cycles.

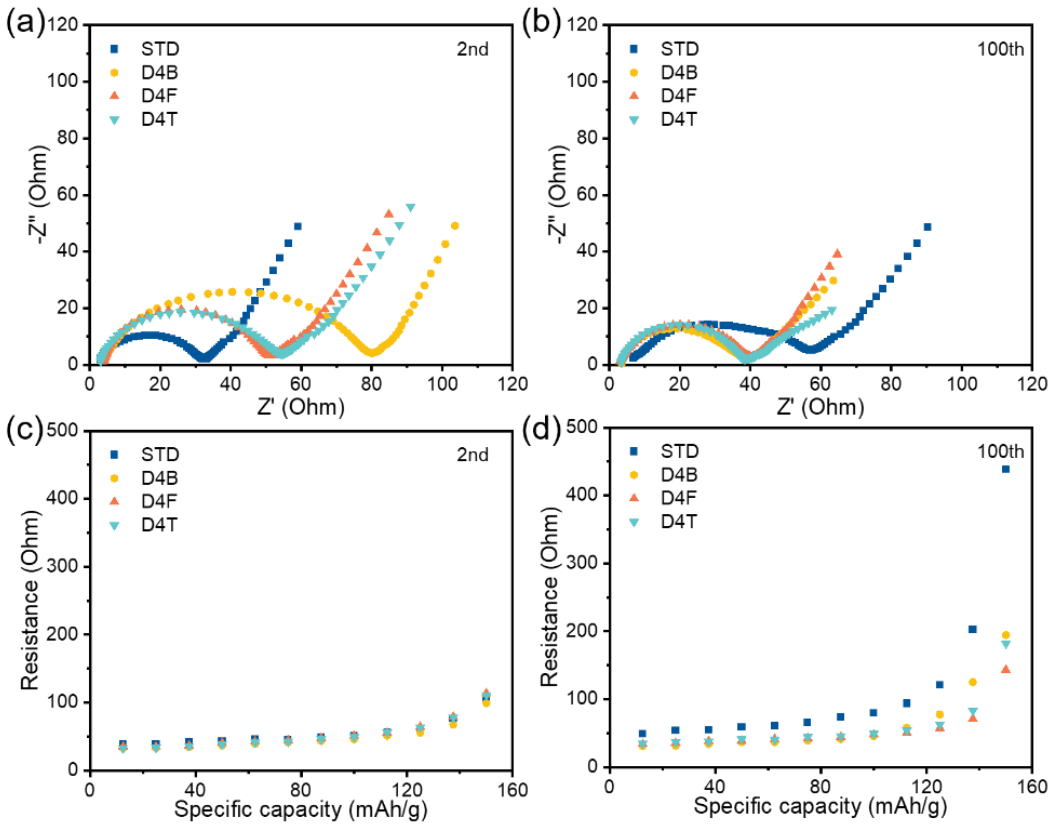

Figure S12. (a, b) AC impedance and (c, d) DC impedance of the Li||LFP cells after (a, c) 2 formation cycles and (b, d) 100 cycles.

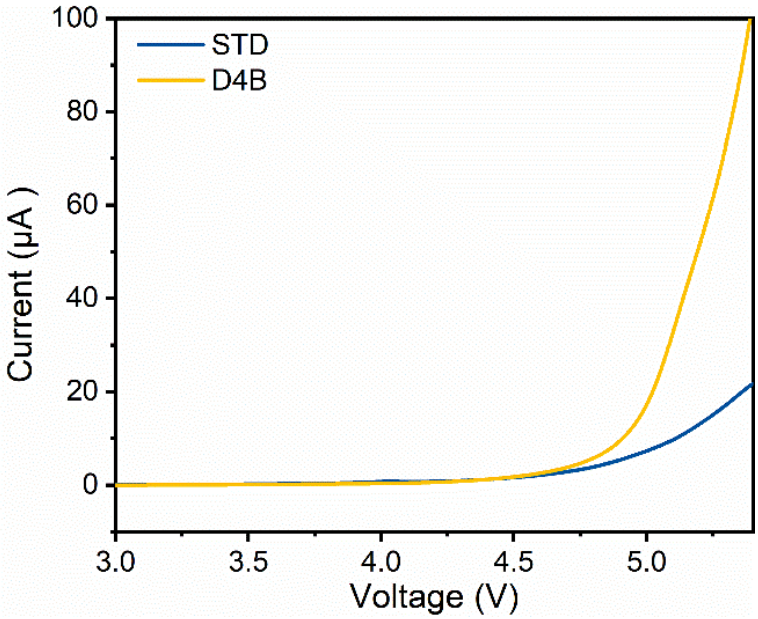

Figure S13. LSV curves of the STD and D4B electrolytes on Pt electrode at a scan rate of 0.5 mV s^{-2}.

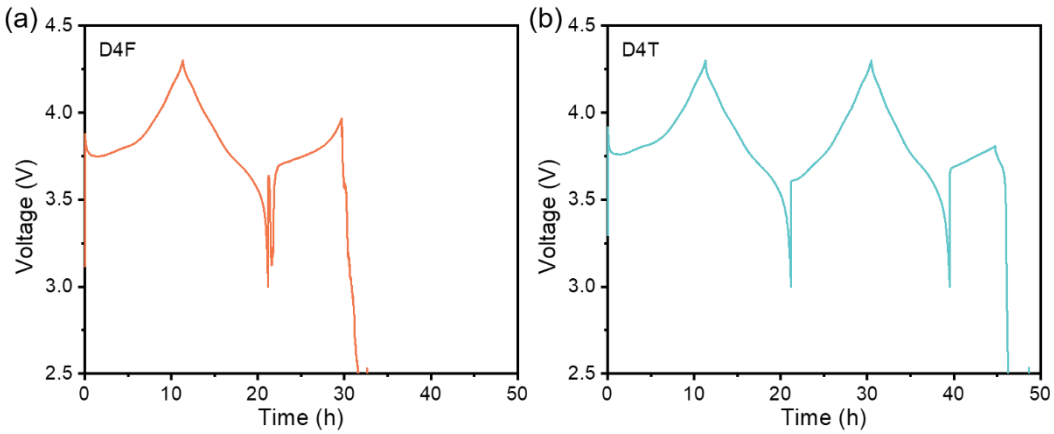

Figure S14. Charge and discharge curves of Li||$LiNi_{0.6}Co_{0.2}Mn_{0.2}O_2$ cells using (a) D4F and (b) D4T electrolytes.

The oxidative stability of D4B is unsatisfactory from the LSV results (Figure S13). The LSV tests reveal that the high voltage stability of D4B is inferior to STD electrolyte, which is mainly attributed to the poor oxidative stability of LiBOB. Since LiFSI and LiTFSI corrode Al foil extensively, the performance of Li||NCM622 cells in D4F and D4T electrolytes is poor

(Figure S14). The results show that the cells can only operate less than 3 cycles. After disassembling the cycled cells, we found that the Al current collector has splintered into pieces, especially in the D4F electrolyte. Thus, 0.1 M LiDFP cannot inhibit the corrosion of Al foil by LiFSI and LiTFSI effectively.